Panax Ginseng combined with platelet rich plasma ameliorates induced benign prostatic hyperplasia in adult albino rats (Histological and Immunohistochemical Study).

ABSTRACT

Background: Benign prostatic hyperplasia (BPH) is a widespread disorder relating to the prostate associated with aging. It affects more than 100 million men worldwide, with a prevalence of approximately 50% after the age of 50 years. Platelet-rich plasma (PRP) has garnered considerable interest as a regenerative curative option for prostatic problems owing to its reparative processes of proliferation-inducing agents that support reparative processes and modulate inflammation. *Panax Ginseng* is widely used in medicine. It is recognized for its multifaceted therapeutic benefits, exhibiting anti-inflammatory, antioxidant, and antiproliferative effects. The present study suggests that their combined use enhances therapeutic outcomes in BPH. **Materials and Methods:** 63 rats were assigned to six groups in a random manner: [control, bisphenol A (BPA), PRP- treated, Ginseng- treated, PRP + Ginseng- treated, and recovery groups]. Prostate samples were gathered and handled for histopathological and immunohistochemical examinations. **Results:** The BPA group illustrated deformed acini, marked stratification, obliterated lumen, significant increases ($P < 0.01$) in fibrosis, PCNA and ER immunoreactivity. Administration of PRP or Ginseng significantly mitigated these changes, as evidenced by marked reductions in fibrosis, PCNA, and ER expression ($P < 0.01$) in comparison with the BPA-treated group. (BPA + PRP + Ginseng group) presented histological architecture closely mirroring that in the control group. **Conclusion:** PRP and *Panax Ginseng* combined therapy greatly enhanced the therapeutic impact on experimentally produced BPH in rats, improving histological architecture and reducing fibrosis.

Key Words: Bisphenol A, Benign prostatic hyperplasia, PRP, Panax Ginseng.

INTRODUCTION

Among elderly men, BPH is a prevalent chronic urinary tract condition. The occurrence of BPH shows a progressive rise as age advances, impacting approximately half of the male population older than 50 years and nearly 80% of those above 70 years [1]. The precise mechanisms responsible for BPH have not been identified. The growth of the prostate is associated with elevated proliferation of epithelial, stromal, and smooth muscle cells which are the most important feature. Men with prostate enlargement frequently develop lower urinary tract symptoms, including urgency, nocturia, painful urination, and interrupted urinary flow, due to urethral compression [2].

Current pharmacological therapies used for BPH involve the use of 5α-reductase inhibitors and α-blockers which represent the first-line treatment for BPH, effectively alleviating urinary symptoms. However, these medications are associated with multiple adverse outcomes encompassing sexual impairments, hypotension, and dizziness [3]. Therefore, considerable effort has been devoted to identifying new therapeutic strategies for BPH that combine effective management with a reduced risk of adverse effects.

Bisphenol A is an artificial hormone disruptor that is widely used to manufacture polycarbonate plastic items [4]. BPA exposure in humans occurs on an ongoing basis through the everyday use of plastic containers, food packaging, and other consumer products. Exposure happens via oral intake, contact with the skin, or inhaling the substance. Its accumulation in the body is linked to endocrine disruption including heightened risk of prostate related pathologies such as BPH [5]. It exerts estrogen-like activity through its interaction with estrogen receptors, thereby influencing gene expression in estrogen-regulated tissues, particularly the prostate [6].

Growing attention has been directed toward new cellular-based therapies within regenerative medicine. It has been applied throughout different medical fields, covering dentistry, orthopedics, dermatology and urology. It refers to an autologous blood fraction in which platelets are concentrated through centrifugation. The therapeutic interest in PRP arises from its capacity to release a spectrum of growth factors, chemotactic proteins, platelet-rich fibrin (PRF), and various cytokines that stimulate cellular activity and enhance vascular support. It demonstrates significant promise in promoting tissue regeneration, reducing inflammation, supporting tissue remodeling,

potentially reducing the need for surgical intervention and shortening recovery time due to its regenerative properties. It may enhance therapeutic outcomes when combined with other pharmacological agents [7, 8].

Among the different ginseng species, *Panax Ginseng* is the one most frequently employed worldwide. *Panax Ginseng* has earned the title of king of herbs. It exhibits a broad spectrum of pharmacological benefits, displaying multiple effects including antibacterial, antioxidant, anticancer, anti-inflammatory and immune-stimulating activities. It is typically regarded as safe, inexpensive and associated with few adverse effects [9]. Ginsenosides are the primary bioactive compounds in ginseng and are responsible for its therapeutic actions. It has been shown to improve prostate pathology in BPH by reducing inflammation and inhibiting fibrosis [10].

Ginseng has been shown to improve prostate pathology associated with BPH, highlighting its potential as a natural or complementary therapy in conjunction with conventional treatment.

This research focused on assessing the combined effect of PRP and *Panax Ginseng* on the prostate focusing on their potential synergistic impact in alleviating pathological changes associated with BPH.

METHODS AND MATERIALS

1. Study design:

This experimental controlled animal study was designed to evaluate the investigated parameters under standardized laboratory conditions.

2. Laboratory animals and Diet:

The experimental model comprised sixty-three male albino rats of adult age, with a mean weight within the range of 180 -200 grams, which were acquired for this research and placed in the Animal Care Facility at Faculty of Veterinary Medicine, Moshtohor, Benha University. Experimental animals were accommodated in appropriately sized Housing units and were provided with a prescribed commercial nutrition along with allowed unrestricted intake of tap water throughout the 2-months experimental duration. Animal handling was performed following approved ethical protocol. The study protocols received approval from the Research Ethical Committee (MD 5-5-

2023) of the Faculty of Medicine, Benha University for the experimental procedures. After a one-week period for animal adaptation, the experiment was conducted from 5 June 2023 to 5 August 2023.

3. Drugs and Chemicals

Bisphenol A:

It is a light-colored crystalline compound of high purity more than 97%, without any odor (CAS No. 80-05-7). and purchased from Sigma-Egypt (500 gm). The drug was prepared in corn oil (used as vehicle), administered orally via tube [11].

Panax Ginseng:

It was obtained as MARNYS® Ginseng 1000 mg capsule from Al-Ezaby Pharmacy (Benha, Egypt). Each capsule contained a standardized extract with 20% total ginsenosides including Rg1, Re, Rf, Rb1, Rb2, Rc, and Rd. The commercially available capsules were prepared in distilled water (used as the vehicle) and administered orally via gavage [9].

Blood sampling and PRP preparation:

The platelet-rich plasma was obtained through a sequential double-spin procedure. Rats' retroorbital veins were used for obtaining blood. Citrate phosphate dextrose-filled vacuum tubes were used to collect the blood. After centrifuging for 10 minutes at a force of 160×g, the superficial layer was carefully moved into a new vacuum tube, yielding platelet poor plasma (PPP) and PRP. The supernatant was centrifuged once more for 15 minutes at 250×g. Plasma with reduced platelet content, forming the upper portion was carefully collected into a new tube, whereas the layer beneath it was retained as platelet-rich plasma (PRP) [7]. PRP was diluted in phosphate-buffered saline (PBS) at a ratio of 1:1, and 0.5 ml was loaded into a sterile insulin syringe for subcutaneous administration [12]. The final platelet concentration in PRP was determined using an automated cell counter, with a minimum threshold of four times the whole blood level. According to the leukocyte count obtained through automated analysis, the preparation was classified as leukocyte- poor PRP (LP-PRP).

Experimental design:

Sixty-three rats were organized into six separate groups through random assignment:

Group I (control: 28 rats): Animals were distributed into 4 groups, each made up of 7 animals as detailed below:

- Subgroup IA: Rats did not receive any treatment.
- Subgroup IB: Rats were given 0.5 ml of corn oil once daily orally via tube for 4 weeks.
- Subgroup IC: Each rat was administered 0.5ml PBS twice weekly subcutaneously for 4 weeks.
- Subgroup ID: Each rat was administered 0.4 ml purified water once daily orally via tube for 4 weeks.

1. **Group II (BPA group: 7 rats):** Rats were given 50 mg/kg BPA was prepared in 0.5ml of corn oil once daily orally via tube for 4 weeks [11].
2. **Group III (BPA+ PRP group: 7 rats):** Rats were given BPA like group II, and thereafter 4 weeks of BPA administration since the experiment began, rats were given 0.5 ml of PRP that had been prepared in PBS at a 1:1 ratio, promptly loaded into a sterilized syringe of insulin, and administered two times per week subcutaneously for 4 weeks [8].
3. **Group IV (BPA+ Ginseng group: 7 rats):** Each rat was administered BPA like group II, and thereafter 4 weeks of BPA administration since the experiment began, rats were treated with Ginseng (200 mg/kg/day) prepared in 0.4 ml purified water once daily orally via tube for 4 weeks [9].
4. **Group V (BPA+ PRP + Ginseng group: 7 rats):** Each rat was administered BPA like group II, and thereafter 4 weeks of BPA administration since the experiment began, rats were given 0.5 ml of PRP as group III and were given Ginseng as group IV in the same day of the first dose of PRP until sacrificed after 8 weeks since the experiment began.
5. **Group VI (recovery group: 7 rats):** Rats were given BPA as mentioned before for 4 weeks, rats in this group were euthanized at the completion of the eight-week experimental period without any treatment.

Ten rats were additionally allocated for the preparation of PRP. it was obtained by using a double-spin procedure. All procedures were carried out at the Lab of Medical Biochemistry, Faculty of Veterinary Medicine, Moshtohor, Benha University.

Sample preparation

Throughout this study period, all animals survived without any fatalities. Rats underwent deep anesthesia with ketamine (100 mg/kg) and xylazine (10 mg/kg) via intramuscular route prior to euthanasia. Group II rats were terminated upon completion of four weeks of the experiment began, while those in groups I, III, IV, V, and VI were euthanized eight weeks post-experiment initiation. Prostate samples were harvested from the ventral lobe of all animals. Each tissue sample was placed in 10% neutral buffered formalin and left for 24–48 hours for fixation. The samples processed through dehydration in a sequential ethanol gradient and and later embedded in blocks of paraffin for sectioning. Tissues of 5–7 µm thickness were cut then prepared and processed for microscopic and immunohistochemical analysis.

Histopathological studies:

H&E and Masson trichrome staining

Prostatic tissues sliced into 5–7 µm thickness, sections positioned on clean microscope slides, stained with H&E evaluated histological alterations, whereas Masson trichrome identified collagen deposition [13].

Immunohistochemical studies:

Immunohistochemical procedures were conducted via a peroxidase-based streptavidin-biotin method. Mounted paraffin sections on positively charged slides underwent deparaffinization, rehydration, and incubation in 0.3% hydrogen peroxide to suppress endogenous peroxidase activity. After incubation in 10% normal rabbit serum for 30 minutes, primary antibodies were applied for 1 hour. Counterstaining of sections was undertaken with Mayer's hematoxylin (product code: TA-060-MH), dehydrated, cleared using xylene and cover slipped with Canada balsam [14].

Proliferating cell nuclear antigen (PCNA) expression was undertaken using a monoclonal antibody derived from mice (product code. MS-106-P, Lab Vision Corporation, Thermo Scientific, Fremont, CA, USA). Positive staining appeared as brown coloration within nuclei within cells undergoing proliferation [14].

Estrogen Receptor (ER) was identified using a mouse monoclonal IgG antibody (code no. M0851, clone 1A4, Dako Life Trade, Egypt), which Furthermore presented as a brown nuclear reaction. Immunohistochemical detection was performed through an avidin–biotin–peroxidase approach. Diaminobenzidine (DAB; Dakopatts, Glostrup, Denmark) was employed as the color-developing agent to visualize antibody binding [15].

All tissue sections were examined under a light microscope at ×400 magnification. Scale bars (30 μm) have been included directly on all photomicrographs to ensure accurate representation of tissue dimensions.

Morphometric Study

Seven microscopic fields were selected randomly and analyzed in a blinded manner to avoid selection bias and to ensure representativeness of the tissue sample. The average proportion of collagen fibers in the tissue (Masson trichrome), PCNA, and ER nuclear staining was determined. For quantification, Image-Pro Plus 6.0 software (Media Cybernetics, Bethesda, MD, USA) was used.

Statistical Analysis

All experimental measurements were recorded, organized, processed, and analyzed using SPSS Statistics for Windows, v.22 (IBM, USA). Morphometric data presented in **(Tables 1, 2, and 3)** were analyzed by one-way ANOVA followed by the Post Hoc LSD test, which was applied consistently across all parameters. Statistical significance was set at $P < 0.01$, and this threshold is explicitly indicated in all figure legends and histograms to facilitate interpretation. Data are expressed as mean ± standard deviation (M ± SD).

RESULTS

Hematoxylin and Eosin stain results:

The different subgroups of group I **(control group)** illustrated comparable microscopic features. Subgroup IA is shown here as a typical example of the reference group. Prostatic sections showed tightly arranged secretory acini of regular uniform morphology, filled with acidophilic prostatic secretions and minimal fibromuscular stroma in interacinar spaces. At higher magnification, the acini were covered with simple cuboidal epithelium with centrally located round nuclei. Acini were filled with acidophilic prostatic secretions **(Fig. 1A&1B).** Group II **(BPA group)** showed the prostatic acini were irregular, distorted, and variable in size, with thickened epithelium, papillary projections, marked stratification, obliterated lumina, degenerative changes, some nuclei showed pyknosis, vacuolated cytoplasm, presence of inflammatory cells along with dilated, engorged blood vessels in interacinar spaces **(Fig. 1C),** group III **(BPA + PRP group)** showed partially thickened epithelium, papillary projections, some acini with pyknotic nuclei and vacuolated cytoplasm, and dilated blood vessels in interacinar spaces **(Fig. 1D),** group IV **(BPA + Ginseng group)** demonstrated areas of thickened epithelium, papillary projections, presence of inflammatory cells along with dilated, engorged blood vessels in interacinar spaces **(Fig. 1E),** group V **(BPA + PRP + Ginseng group)** exhibited nearly normal, regular acini lined by simple cuboidal epithelial cells exhibiting rounded nuclei, containing acidophilic secretions, with visible blood vessels in interacinar spaces **(Fig. 1F),** group VI **(recovery group)** showed irregular prostatic acini were lined with thickened epithelium, papillary projections, stratification with narrow lumen and blood vessels were observed in interacinar spaces **(Fig. 1G).**

Masson trichrome staining results:

Prostatic sections showed minimal collagen deposition in group I **(control group) (Fig. 2A)** and in group V **(BPA + PRP + Ginseng group) (Fig. 2E).** Intense accumulation was observed in group II **(BPA group) (Fig. 2B)**, mild in group III **(BPA + PRP group) (Fig. 2C)**, and moderate in group IV **(BPA + Ginseng group) (Fig. 2D).** Group VI **(recovery group) (Fig. 2F)** exhibited marked collagen deposition. A histogram presenting the average collagen fiber content across all experimental groups is provided in **(Fig. 2G).**

Anti PCNA staining results:

Prostatic sections showed low PCNA-positive nuclear immunoreactivity in group I **(control group) (Fig. 3A)** and group V **(BPA + PRP + Ginseng group) (Fig. 3E).** Intense PCNA expression was observed in group II **(BPA group) (Fig. 3B),** while mild immunoreactivity was noted in group III **(BPA + PRP group) (Fig. 3C)** and moderate in group IV **(BPA + Ginseng group) (Fig. 3D)**, respectively. In contrast, group VI **(recovery group) (Fig. 3F)** exhibited marked PCNA-positive nuclei. A histogram presenting the average PCNA immunoreactive area for all groups is provided in **(Fig. 3G).**

Anti ER staining results:

Prostatic sections showed minimal ER-positive nuclear immunoreactivity in Group I **(control group) (Fig. 4A)** and Group V **(BPA + PRP + Ginseng group) (Fig. 4E).** Intense ER immunostaining appeared in Group II **(BPA group) (Fig. 4B),** while mild immunoreactivity was noted in Group III **(BPA + PRP group) (Fig. 4C)** and moderate in Group IV **(BPA + Ginseng group) (Fig. 4D)**, respectively. In contrast, group VI **(recovery group) (Fig. 4F)** exhibited marked ER-positive nuclei. A histogram presenting the average ER immunoreactive area for all groups is provided in **(Fig. 4G).**

Morphometric and Statistical Results:

Mean values ± standard deviation (SD) of collagen fiber accumulation, along with PCNA and ER immunoreactivity, across all experimental groups are summarized in **(Tables 1,2,3)** and illustrated in **(Histograms 1,2,3)**. Groups III, IV, and V displayed significantly lower levels ($P < 0.01$) of collagen accumulation, PCNA, and ER immunoreaction relative to groups II and VI. In contrast, groups II and VI showed a marked increase ($P < 0.01$) in these measurements relative to the remaining groups.

Morphometric data are presented in both tabular and graphical formats. Values reported in the text, tables, and histograms are identical and expressed to three significant figures to ensure consistency and data integrity.

DISCUSSION

Benign prostatic hyperplasia is a common abnormal prostatic disease that can cause problems with the lower urinary tract, which may lead to cancerous diseases like prostate cancer. Therefore, finding new ways to treat prostatic disorders is crucial [8].

Recently, BPA has attracted global attention because it interferes with the endocrine system. Bisphenol A causes numerous problems for the body, particularly affecting the male reproductive system [16].

The mechanism underlying BPA-induced BPH was described by Nguyen et al. 2022 [6]. BPA belongs to a group of environmental estrogens. It interacts with estrogen receptors, affecting the way in which genes controlled by estrogen are expressed and raising the ratio of estrogen to androgen. Also, Sanchez et al. 2022 [4] reported that BPA enhances the synthesis of dihydrotestosterone due to its estrogenic properties, drives cellular proliferation, and increases prostaglandin D2 synthase.

Moreover, Bleak et al. 2021 [17] noted that BPA caused epithelial mesenchymal transition (EMT), which resulted in the proliferation of prostate tissue. In addition, immotile epithelial cells can also become motile mesenchymal cells through EMT. Mesenchymal-like cells generated from the prostatic epithelium accumulate, and stromal cells proliferate in BPH.

Group II (BPA group) in the present study showed irregular, distorted acini of variable size, thickened epithelium, papillary projections, marked stratification with obliterated lumen, some acinar cells had pyknotic nuclei with vacuolated cytoplasm, presence of inflammatory cells along with expanded and engorged vasculature in interacinar spaces. There was a substantial increase in collagen fiber accumulation, as well as in PCNA and ER immunostaining relative to the control group, which was considered significant at ($P < 0.01$). These outcomes are similar to those reported previously that showed variable-sized, disorganized acini, thickening of the epithelium, hyperplasia, obliterated lumen, papillary projections, congested dilated blood vessels, and inflammatory cellular infiltration were all features of the prostatic tissue [16, 18-21].

These pathological observations were described by numerous researchers who stated that bisphenol A increases nitric oxide levels, decreases antioxidant enzymes, and produces excessive

hydrogen peroxide, which is harmful to the prostate. It also disrupts the equilibrium between prostate cell growth and apoptosis in prostate cells, leading to BPH development. Bisphenol A also accumulates in the endoplasmic reticulum, disrupts protein synthesis, and prevents the formation of apoptosis inhibitors such as B-cell leukemia/lymphoma 2 protein. Furthermore, BPA alters the activities of ATPase in cells and leads to a decrease in ATP production which causes cellular necrosis and damage [8, 22-27].

Furthermore, Ibrahem et al. 2022 [8] stated that BPA alters estrogen-mediated signaling cascades and affects the transcriptional activity of associated target genes. The nuclear receptor family includes estrogen receptors which play a role in transcription control. Within the nucleus, bisphenol A engages ERα and binds to defined DNA response elements, leading to the activation of target genes. This association upregulates ERα expression and drives cell growth.

Moreover, Nasr et al. 2021 [9] reported that BPA accumulates in mitochondria, cytochrome c is released, mitochondrial malfunction occurs, and lipid peroxidation is induced, which activates endonuclease enzymes and damages DNA. Reactive oxygen species damage cell membranes, organelles, causing the dissolution of cytoplasm due to their cytotoxic capacity. Lysosomal rupture releases hydrolytic enzymes in the cytoplasm.

In addition, Meli et al. 2020 [28] stated that acinar cells have pyknotic nuclei as a result of pyroptosis (programmed necrosis), an inflammatory response that triggers caspase 1 and causes nuclear condensation, cellular ionic gradient breakdown and membrane pore development.

Also, Nasr et al. 2021 [9] stated that when cells go through pyroptosis, they release proinflammatory mediators that cause inflammation and encourage the development of mesenchymal and epithelial cell components. The inflammatory response is defined by infiltration of immune cells mediated by free radicals, along with vascular dilation and congestion, which together enhance blood flow to degenerating tissues.

Moreover, Awad et al. 2024 [29] reported that oxidative stress promotes fibroblast activity, promotes collagen deposition, and improves extracellular matrix production. Benign prostatic hyperplasia is the cause of mast cell activation. Inflammation and fibrosis are dependent on mast cells. Profibrotic and inflammatory mediators are released as a result of their activation and

degranulation. Additionally, tissue fibrosis is promoted by cytokine production which stimulates fibroblast differentiation into myofibroblasts.

Also, Ibrahem et al. 2022 [8] stated that PCNA is regarded as a crucial marker for identifying DNA synthesis and cell proliferation. Increased PCNA levels also indicate a high rate of cell division. It is a nuclear protein that was produced in the early S and late G1 stages. Any defect in DNA function results in aberrant nuclear membranes and increased PCNA expression in BPH prostatic tissues.

After 8 weeks, group III (BPA + PRP group) showed parts of prostatic acini lined with thickened epithelium, papillary projections, some acini had pyknotic nuclei with vacuolated cytoplasm and dilated blood vessels were observed in interacinar spaces. In relation to groups II, IV, and VI, there was a statistically significant ($P < 0.01$) reduction in collagen fibers and immunoreaction for PCNA and ER. These findings agree with the results of many researchers who reported that PRP treatment has a significant therapeutic impact due to its antioxidant, antifibrotic and anti-inflammatory features. It also contains numerous leukocytes, thereby lowering cell proliferation, as these leukocytes emit proinflammatory chemicals during the degranulation process, inhibiting cell proliferation. In addition, PRP is enriched with a high level of growth-promoting factors that promote immunity and encourage cell death leading to inhibition of proliferation [8, 30-34].

Moreover, Dos Santos et al. 2021 [30] stated that platelets that produce growth factors are abundant in PRP. Formation of reactive oxygen species and free radicals is reduced, as well as antioxidant enzyme activity, particularly glutathione peroxidase, is increased by these growth factors. Additionally, it functions as an apoptotic regulatory messenger by inhibiting the production of the kinase 1 signal which controls differentiation, proliferation and apoptosis.

Furthermore, Braczkowski et al. 2024 [34] described that Transforming growth factor beta (TGF-β) limits DNA synthesis and restricts cell enhancement by blocking the G1–S cell cycle progression regulated through the cyclic adenosine monophosphate response element-binding protein and by suppressing the production of mitogenic growth factors. TGF-β serves as a powerful suppressor of epithelial cell growth, affecting both normal and abnormal cells, and is believed to function as anticancer regulatory protein by promoting programmed cell death and limiting cell proliferation.

Moreover, Deng et al. 2024 [35] stated that PRP reduces inflammation by disrupting the nuclear factor kappa B signaling cascade and proinflammatory cytokine expression. It has antifibrotic properties that limit the fibroblast-myofibroblast transition and reduce collagen deposition which encourages fibroblast death.

After 8 weeks, group IV (BPA + Ginseng group) showed parts of prostatic acini lined with thickened epithelium, papillary projections, presence of inflammatory infiltrates and engorged, dilated blood vessels in interacinar spaces. There was a significant reduction ($P < 0.01$) in collagen fibers deposition as well as PCNA and ER immunostaining relative to group II, VI and this evidence supports prior studies reporting that *panax Ginseng* has anti-proliferative action, which is mediated through telomerase suppression that shortens telomeres, resulting in cell death which alleviates many pathological signs. By promoting caspase activity or inhibiting mitogen activated protein kinase signaling pathways, ginseng induces cell arrest. Furthermore, Ginseng suppresses androgen receptor (AR) and 5α-reductase activity in prostate tissues which controls AR-mediated proliferation [2, 9, 36-38].

Furthermore, El-Demerdash et al. 2021 [37] stated that Ginseng has an antioxidant action by reducing harmful reactive oxygen species and raising the functional activity of key antioxidant enzymes, encompassing glutathione peroxidase, catalase, and superoxide dismutase. Moreover, Ginseng reduces inflammation by suppressing the proinflammatory cytokines such as chemokines, nitric oxide, interleukin 8 and cyclooxygenase 2. Additionally, it exerts anti-fibrotic effects by inhibiting active myofibroblasts and encouraging the extracellular matrix to break down by upregulating matrix metalloproteinase enzymes.

After 8 weeks, group V (BPA + PRP + Ginseng group) showed nearly normal regular acini lined by simple cuboidal epithelial cells exhibiting rounded nuclei, acini contained acidophilic prostatic secretions and blood vessels could be seen in interacinar spaces. A marked decline ($P < 0.01$) in the accumulation of collagenous fibers was observed as well as in PCNA and ER immunoreaction relative to group II, III, IV, VI and the current data corroborate the outcomes of Zaazaa et al. 2020 (39) who documented that PRP releases numerous growth-promoting factors and bioactive protein molecules that attract macrophages and facilitate the phagocytosis process, which removes necrotic tissue. Also, the agonistic and antagonistic growth factors in PRP aid in reducing fibrosis

and inflammation. When administered alongside drugs with antioxidant and anti-inflammatory effects, this approach reduces inflammation and mitigates oxidative stress. The observed improvements in histology and immunostaining are likely due to the antioxidant and anti-inflammatory properties provided by PRP and other therapeutic compounds**.**

Furthermore, Ebrahim et al 2022 [40] stated that groups treated with cinnamon and PRP, the pancreatic tissues demonstrated significant improvements in the lobular architecture as well as a restoration of the volume and distribution of islet cells. The pancreatic histoarchitecture was remarkably restored in both combination therapy groups. In line with this, the present findings suggest that the combined administration of Ginseng and PRP appears to exert a dual protective effect. Ginseng mediates antiproliferative activity through suppression of androgen receptor signaling, thereby limiting abnormal cellular proliferation. The antifibrotic properties of PRP, achieved through inhibition of TGF-β signaling and suppression of myofibroblast differentiation, act in concert with the antiproliferative effects of Ginseng, mediated by telomerase inhibition and androgen receptor regulation. This combined mechanism effectively limits stromal fibrosis while restraining epithelial hyperplasia, thereby accounting for the superior therapeutic outcomes observed in Group V compared with either treatment alone.

After 8 weeks, group VI (recovery group) showed prostatic acini lined with thickened epithelium, papillary projections, stratification with narrow lumen. Accumulation of inflammatory cells alongside vascular dilation and congestion in interacinar spaces persisted in the recovery group. In relation to the control group, the levels were significantly elevated ($P < 0.01$) in collagen fibers deposition as well as PCNA and ER immunoreaction. In relation to group II, PCNA and ER immunoreactivity were significantly reduced ($P < 0.01$), while collagen fibers showed a slight reduction that was not statistically significant. The observed results are consistent with previous studies that demonstrated that BPA mediates harmful alterations in the prostate, and these changes are not fully reversed upon withdrawal of BPA because of the lipid-soluble nature of BPA, which allows its accumulation in adipose tissue at higher concentrations. Its metabolism is modulated by factors such as age, gender and liver function [16, 41-42].

Moreover, Dees et al. 2021 [43] reported that upon disruption of regulatory mechanisms, fibroblasts persist in an activated state, so there is partial recovery of the prostate that occurs when BPA treatment is stopped.

On the other hand, Cao et al. 2020 [44] observed that BPA toxicity was reversible at low doses 0.05 and 5 mg/kg, whereas exposure to a high dose (50 mg/kg) resulted in irreversible damage. This indicates that higher concentrations of BPA can cause permanent damage.

CONCLUSION

Histological and immunohistochemical analysis showed that BPA induced marked alterations in prostatic tissue including epithelial hyperplasia, distorted acini, inflammatory infiltration, vascular congestion, and increased collagen deposition. Treatment with PRP or *Panax Ginseng* improved these pathological changes, while combined administration of PRP and *Panax Ginseng* resulted in the most pronounced restoration of tissue architecture, reduction of fibrosis, and decreased proliferative markers.

RECOMMENDATION

Future studies should combine functional, biochemical and histological assessments, and investigate different dosages and treatment durations of PRP and *Panax Ginseng* to optimize their effects on BPH repair.

SOURCES OF FUNDING

The authors did not receive any financial support.

AUTHOR CONTRIBUTION

Each author contributed equally to the present work.

CONFLICTS OF INTEREST

The study was carried out independently.

REFERENCES

1. Siqueira, M. H. B. Risk factors for benign prostatic hyperplasia: a comprehensive review. Revista da Associacao Medica Brasileira. (2025); 71(6): 1-5. DOI:10.1590/1806-9282.20250343.

2. Park, J. Y.; Park, W. Y.; Song, G.; Jung, S. J.; Kim, B.; Choi, M. et al. *Panax ginseng* C.A. meyer alleviates benign prostatic hyperplasia while preventing finasteride-induced side effects. Frontiers in Pharmacology. (2023);14, 1-12. DOI: 10.3389/fphar.2023.1039622.

3. Halawani, A.; Paterson, R.; Zhong, T.; Du, K.; Ren, R.; Forbes, C. Risks and side effects in the medical management of benign prostatic hyperplasia. Prostate International. (2024), 12, 57–64. DOI: 10.1016/j.prnil.2023.11.004.

4. Sanchez, P.; Castro, B.; Martinez-Rodriguez, S.; Rios-Pelegrina, R.; Del Moral, R. G.; Torres, J. M. et al. Impact of chronic exposure of rats to bisphenol A from perinatal period to adulthood on intraprostatic levels of 5α-reductase isozymes, aromatase, and genes implicated in prostate cancer development. Environmental research. (2022); 212, 1-10. DOI: 10.1016/j.envres.2022.113142.

5. Manzoor, M. F.; Tariq, T.; Fatima, B.; Sahar, A.; Tariq, F.; Munir, S. et al. An insight into bisphenol A, food exposure and its adverse effects on health: A review. Frontiers in Nutrition. (2022); 9, 1-16. DOI:10.3389/fnut.2022.1047827.

6. Nguyen, J. L.; Ricke, E. A.; Liu, T. T.; Gerona, R.; MacGillivray, L.; Wang, Z. et al. A. Bisphenol-A analogs induce lower urinary tract dysfunction in male mice. Biochemical Pharmacology. (2022); 197, 1-19. Doi.org/10.1016/j.bcp.2021.114889.

7. Ebrahim, N.; Dessouky, A.A.; Mostafa, O.; Hassouna, A.; Yousef, M.M.; Seleem, Y. et al. Adipose mesenchymal stem cells combined with platelet-rich plasma accelerate diabetic wound healing by modulating the Notch pathway. Stem Cell Research & Therapy. (2021); 12(1):392. DOI:10.1186/s13287-021-02454-y.

8. Ibrahem, N.; Elsadek, A.; Selim, A. and Selim, S. Ameliorating the effect of platelet-rich plasma on histological and biochemical changes induced by bisphenol A in prostate of adult albino rats. Egyptian Journal of Histology. (2022); 45(1): 240-259. DOI. org/10.21608/ejh.2021.56355.1412.

9. Nasr, S.; Moustafa, M.; Boughdady, W. and Yousry, M. A histological study of the effect of *panax Ginseng* versus finasteride on induced benign prostatic hyperplasia in rats with potentiality of spontaneous recovery. Egyptian Journal of Histology. (2021); 44(3): 587-600. DOI.org/10.21608/ejh.2020.43908.1360.

10. He, R.; Tian, D.; Yang, Y.; Chen, C.; Li, L.; Lee, Y.J. Pharmacological efficacy of ginseng on gender-specific benign reproductive diseases. Innovations in Acupuncture and Medicine. (2025); 18(1):4. DOI:10.1186/s44424-025-00004-4.

11. Mahmoud, A.; seliem, A.; Selim, S. and Ibrahem, N. The sensitivity of adult male albino rat prostate to low-dose bisphenol A: A histological and immunohistochemical study. Zagazig University Medical Journal. (2021); 9(2): 1-12. DOI: 10.21608/zumj.2021.66437.2163.

12. Rania, N. A.; Islam. I. H. and Atef, M. M. Effect of Platelet-rich plasma on an experimental rat model of Adriamycin induced chronic kidney disease. Medical Journal of Cairo University. (2019); 87(3): 2207-2217. DOI: 10.21608/mjcu.2019.54382.

13. Bancroft, J. D. and Layton. C. The hematoxyline and eosin and Connective and other mesenchymal tissues with their stains Techniques. Eds. Suvarna, S. K.; Layton, C. and Bancroft, J. D. 8th ed. Ch.10& 12. (2019); Pp. 126-138& 153-175. Churchill Livingstone of El Sevier, Philadelphia. ISBN: 978-0-7020-6864-5.

14. Jackson, P. and Blythe, D. Immunohistochemical techniques. Theory and practice of histological techniques. Eds. Suvarna, S. K., Layton, C., and Bancroft, J. D. 7th edition. Chapter 17. (2013): Pp. 381-426. Churchill Livingstone, Elsevier, Philadelphia. ISBN: 978-0-7020-4226-3.

15. Charafe-Jauffret, E.; Tarpin, C.; Bardou, V. J.; Bertucci, F.; Ginestier, C.; Braud, A. C.et al. Immunophenotypic analysis of inflammatory breast cancers: Identification of an inflammatory signature. Journal of Pathology. (2004); 202(3): 265–273. DOI.org/10.1002/path.1515.

16. Aziz, J. and Moawad, R. Harmful impacts of bisphenol A on the prostate of adult albino rat and the possible role of recovery: Histological and Immunohistochemical study. Journal of Medical Histology. (2021); 5(2): 105-118.

17. Bleak, T. C. and Calaf, G. M. Breast and prostate glands affected by environmental substances.Oncology Reports. (2021); 45(4): 20-38. DOI.org/10.3892/or.2021.7971.

18. Mustafa, M. M.; Anani, R, A.; Aly, M, A. and Mansy, M. I. Allogeneic injectable platelet rich plasma improves neurotization index in a rat model.. Zagazig University Medical Journal. (2022); 28(6): 50-57. DOI: 10.21608/zumj.2019.18582.1602.

19. Wu, S.; Huang, D.; Su, X.; Yan, H.; Wu, J. and Sun, Z. Oral exposure to low dose bisphenol A induces hyperplasia of dorsolateral prostate and upregulates EGFR expression in adult sprague dawley rats. Toxicology and Industrial Health. (2019); 35(10): 647–659. DOI.org/10.1177/0748233719885565.

20. Zhang, M.; Luo, C.; Cui, K.; Xiong, T. and Chen, Z. Chronic inflammation promotes proliferation in the prostatic stroma in rats with experimental autoimmune prostatitis: Study for a novel method of inducing benign prostatic hyperplasia in a rat model. World Journal of Urology. (2020) 38(11): 2933-2943. DOI.org/10.1007/s00345-020-03090-6.

21. Tang, X.; Liu, Z.; Ren, J.; Cao, Y.; Xia, S.; Sun, Z. et al. Comparative RNA-sequencing analysis of the prostate in a mouse model of benign prostatic hyperplasia with bladder outlet obstruction. Molecular and Cellular Biochemistry. (2023); 478(12): 2721–2737. DOI.org/10.1007/s11010-023-04695-2.

22. Huang, D. Y.; Zheng, C. C.; Pan, Q.; Wu, S. S.; Su, X.; Li, L. et al. Oral exposure of low dose bisphenol A promotes proliferation of dorsolateral prostate and induces epithelial-mesenchymal transition in aged rats. Scientific Reports. (2018); 8(1): 490-500. DOI.org/10.1038/s41598-017-18869-8.

23. Jin, B. R.; Cheon, S. Y.; Kim, H. J.; Kim, M. S.; Lee, K. H. and An, H. Anti-proliferative effects of standardized cornus officinalis on benign prostatic epithelial cells via the PCNA/E2F1dependent cell cycle pathway. International Journal of Molecular Sciences. (2020); 21(24): 1-15. DOI.org/10.3390/ijms21249567.

24. Maczka, W.; Grabarczyk, M. and Winska, K. Can antioxidants reduce the toxicity of bisphenol? Antioxidants International Journal. (2022); 11(2): 413-432. DOI.org/10.3390/antiox11020413.

25. Rasheed, R. A.; Sadek, A. S.; Khattab, R. T.; Elkhamisy, F. A.; Abdelfattah, H. A.; Elshaer, M. M. et al. Diacerein provokes apoptosis, improves redox balance, and downregulates PCNA and TNF-α in a rat model of testosterone-induced benign prostatic hyperplasia: A new non-invasive approach. Public Library of Science. (2023); 18(11): 1-18. DOI.org/10.1371/journal.pone.0294972.

26. Saleh, S. M.; Mahmoud, A. B.; Al-Salahy, M. B. and Mohamed, F. A. Morphological, immunohistochemical, and biochemical study on the ameliorative effect of gallic acid against bisphenol A-induced nephrotoxicity in male albino rats. Scientific Reports. (2023); 13(1), 1732-1752. DOI.org/10.1038/s41598-023-28469-2.

27. Wang, Z.; Mao, Q.; Yuan, Y.; Wang, C. and Wei, H. Shuangshi Tonglin capsule treats benign prostatic hyperplasia through the ROS/NLRP3 signaling pathway. International Urology and Nephrology. (2023); 56(4): 1259-1271. DOI.org/10.1007/s11255-023-03874-w.

28. Meli, R.; Monnolo, A.; Annunziata, C.; Pirozzi, C. and Ferrante, M. C. Oxidative Stress and BPA Toxicity: An Antioxidant Approach for Male and Female Reproductive Dysfunction. Antioxidants. (2020); 9(5): 405-422. DOI.org/10.3390/antiox9050405.

29. Awad, N. N.; Mohammed, M. H.; Mahmoud, O. M. and Almallah, A. A. W. Role of Alpha-lipoic acid and Naringin in Modulating Bisphenol-A Induced Perturbations of Prostate in Adult Rats (Histological and Immunohistochemical Study). Egyptian Journal of Histology. (2024); 47(3): 1138-1156. DOI.org/10.21608/ejh.2023.224814.1925

30. Dos Santos, R. G.; Santos, G. S.; Alkass, N.; Chiesa, T. L.; Azzini, G. O.; Da Fonseca, L. F. et al. The regenerative mechanisms of platelet-rich plasma. Cytokine. (2021); 144, 1-8. DOI. 10.1016/j.cyto.2021.155560.

31. Lu, J. H.; Chueh, K. S.; Juan, T. J.; Mao, J. W.; Lin, R. J.; Lee, Y. C. et al. Effects of therapeutic platelet rich plasma on overactive bladder via modulating hyaluronan synthesis in ovariectomized rat. International Journal of Molecular Sciences. (2023); 24(9): 8242-8276. DOI. 10.3390/ijms24098242

32. Tai, H. C.; Tsai, W. K.; Chang, M. L.; Praveen Rajneesh, C.; Tseng, X. W.; Hsu, W. C. et al. Intracavernous injection of platelet-rich plasma reverses erectile dysfunction of chronic cavernous nerve degeneration through reduction of prostate hyperplasia evidence from an aging-induced erectile dysfunction rat model. Federation of American Societies for Experimental Biology Journal. (2023); 37(4): 1-15. DOI.org/10.1096/fj.202201443R.

33. Han, C.; Chen, C.; Lu, N.; Xue, L.; Xing, D.; Wu, W. et al. Platelet-rich plasma inhibits breast cancer proliferation. Clinical Medicine Insights. (2024); Oncology, 18, 1-8. DOI.org/10.1177/11795549241298978.

34. Braczkowski, M. J.; Kufel, K. M.; Kulinska, J.; Czyz. D. L.; Dittmann, A.; Wiertelak, M. et al. Pleiotropic action of TGF beta in physiological and pathological liver conditions. Biomedicines. (2024); 12(4): 925-949. DOI.org/10.3390/biomedicines12040925.

35. Deng, Z.; Fan, T.; Xiao, C.; He, T.; Zheng, Y.; Li, C. et al. TGF-β signaling in health, disease and therapeutics. Signal Transduction and Targeted Therapy. (2024); 61 (9):1-25. DOI.org/10.1038/s41392-024-01764-w

36. Li, X.; Mo, N. and Li, Z. Ginsenosides: Potential therapeutic source for fibrosis-associated human diseases. Journal of Ginseng Research. (2020); 44(3): 386-398. DOI: 10.1016/j.jgr.2019.12.003

37. El-Demerdash, F. M.; El-Magd, M. A. and El-Sayed, R. A. *Panax Ginseng* modulates oxidative stress, DNA damage, apoptosis and inflammation induced by silicon dioxide

nanoparticles in rats. Environmental Toxicology. (2021); 36(7): 1362–1374. DOI: 10.1002/tox.23132

38. Gill, N. B.; Dowker-Key, P. D.; Hubbard, K.; Voy, B. H.; Whelan J.; Hedrick, M. et al. Ginsenoside Rc from *Panax Ginseng* ameliorates palmitate-induced UB/OC-2 cochlear cell injury. International Journal of Molecular Sciences. (2023); 24(8):7345-7366. DOI: 10.3390/ijms24087345.

39. Zaazaa, A. M. and Aniss, N. N. The role of platelet rich plasma and quercetin in alleviating dimethyl nitrosamine induced acute spleen injury through regulating oxidative stress, inflammation and apoptosis. International Journal of Pharmacy and Pharmaceutical Sciences. (2020); 12(5): 1-9. DOI: 10.22159/ijpps.2020v12i5.11927.

40. Ebrahim, U.; Morsi, A.; Fouad, H. and Faruk, E. Pancreatic protection elicited by platelet-rich plasma and cinnamon combination in a rat model of type 1 diabetes: Is it a new era in islet cell regeneration and insulin signalling genes. Egyptian Journal of Histology. (2022); 45(3): 720-737. DOI: 10.21608/ejh.2022.174083.

41. Mohamed, D. A. and Arafa, M. H. Testicular toxic changes induced by bisphenol A in adult albino rats a histological, biochemical and immunohistochemical study. Egyptian Journal of Histology. (2013); 36(1): 233-245. DOI: 10.1097/01.EHX.0000426163.95597.40.

42. Soliman, M.; Noya, D. Effect of Bisphenol A on the lung of adult male albino rats and the possible protective role of propolis: Light and electron microscopic study. Egyptian Journal of Histology. (2023); 46(1): 290-307. DOI: 10.21608/ejh.2021.83475.1515.

43. Dees, C.; Chakraborty, D. and Distler, J. H. W. Cellular and molecular mechanisms in fibrosis. Experimental Dermatology. (2021); 30(1), 121–131. DOI: 10.1111/exd.14169.

44. Cao, T.; Cao, Y.; Wang, H.; Wang, P.; Wang, X.; Niu, H. et al. The effect of exposure to bisphenol A on spermatozoon and the expression of tight junction protein occludin in male mice. International Dose Response Hormesis Society. (2020); 18(2): 1-6. DOI. 10.21608/ejh.2022.174083.

Table (1): Showing the mean area %, SD of collagen fibers deposition in groups I, II, III, IV, V and VI with comparison between all groups by Post Hoc LSD test.

	Group I (Control)	Group II (BPA)	Group III (BPA+PRP)	Group IV (BPA+Ginseng)	Group V (BPA+PRP+Ginseng)	Group VI (Recovery)
Mean area %	0.27%	12.35%**	1.63%**	4.69%**	0.77%**	12.26%**
SD±	0.0141	0.6231	0.1533	0.2046	0.1033	0.2555

** Significant compared to Group I (Control) at $P < 0.01$, no star = non-significant.

Table (2): Showing the mean area %, SD of PCNA immunoreaction in groups I, II, III, IV, V and VI with comparison between all groups by Post Hoc LSD test.

	Group I (Control)	Group II (BPA)	Group III (BPA+PRP)	Group IV (BPA+Ginseng)	Group V (BPA+PRP+Ginseng)	Group VI (Recovery)
Mean area %	0.11%	8.11%**	1.38%**	2.02%**	0.36%**	4.64%**
SD±	0.0191	0.1179	0.0626	0.0451	0.0496	0.2558

** Significant compared to Group I (Control) at $P < 0.01$, no star = non-significant.

Table (3): Showing the mean area %, SD of ER immunoreaction in groups I, II, III, IV, V and VI with comparison between all groups by Post Hoc LSD test.

	Group I (Control)	Group II (BPA)	Group III (BPA+PRP)	Group IV (BPA+Ginseng)	Group V (BPA+PRP+Ginseng)	Group VI (Recovery)
Mean area %	0.16%	4.09%**	1.62%**	2.87%**	1.29%**	3.89%**
SD±	0.0241	0.2012	0.1196	0.1467	0.0844	0.1309

** Significant compared to Group I (Control) at $P < 0.01$, no star = non-significant.

GI (control group)

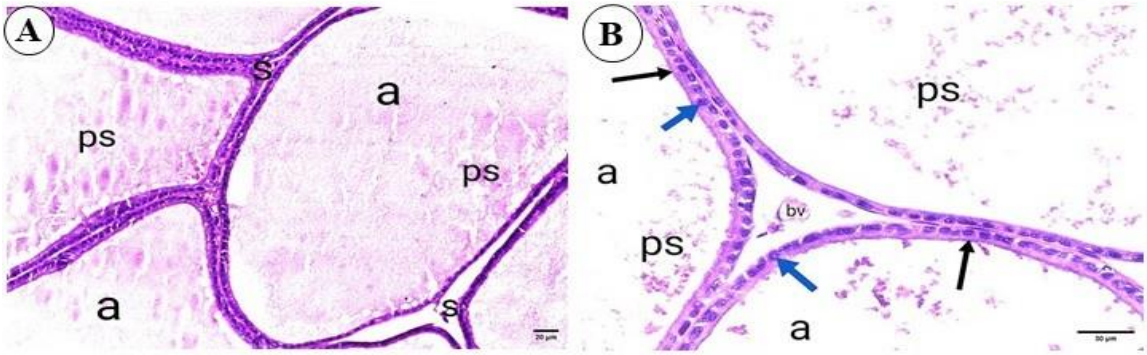

GII (BPA group)

GIII (BPA+PRP group)

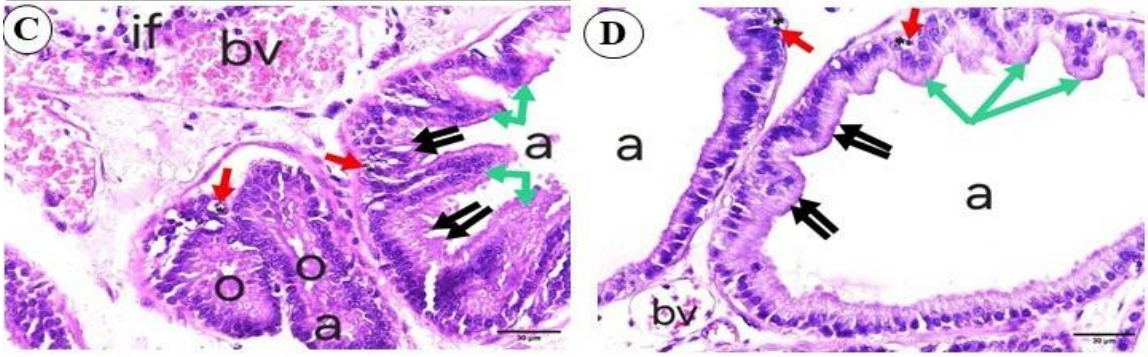

GIV (BPA+ Ginseng group)

GV (BPA+ PRP+ Ginseng group)

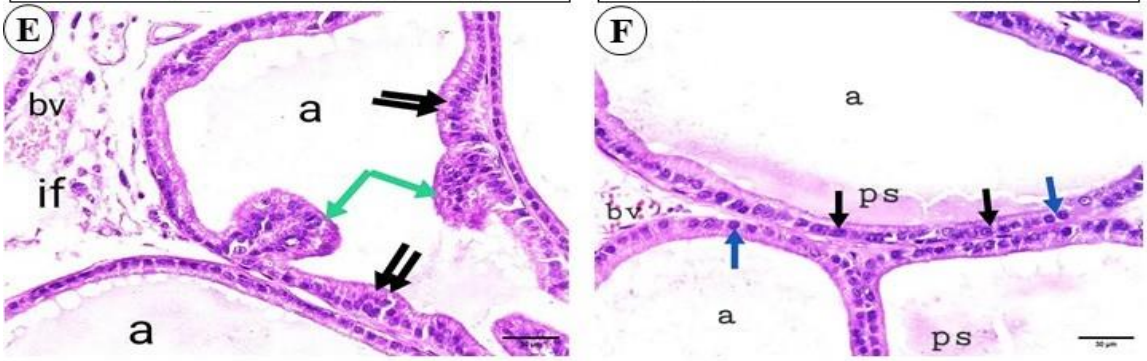

GVI (Recovery group)

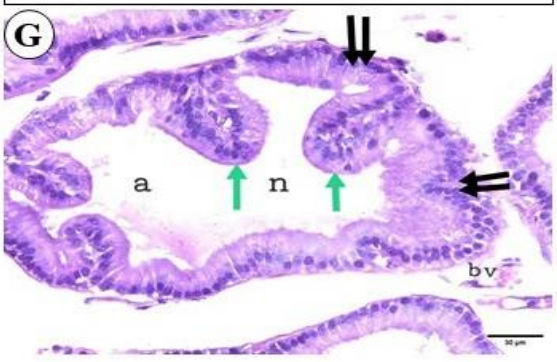

Fig. 1: Photomicrographs of rat prostatic sections stained by H&E: (A): Group I showing normal histological architecture of the prostatic tissue. Closely packed secretory acini **(a)** of regular size and shape. Acini are filled with acidophilic prostatic secretions **(ps)**. Minimal fibromuscular stroma **(s)** in interacinar spaces **(H&E X200), (B):** High magnification of the same group revealing regular acini **(a)** are lined by simple cuboidal epithelium **(black arrow)** with rounded nuclei **(blue arrow)**. Acini are filled with acidophilic prostatic secretions **(ps)**, **(C):** Group II showing irregular distorted variable size acini **(a)**, thickened epithelium **(double arrows),** papillary projections **(green arrows),** marked stratification with obliterated lumen **(o),** some acinar cells have pyknotic nuclei**(red arrow**) with vacuolated cytoplasm **(***), inflammatory cellular infiltration **(if)** and dilated congested blood vessels **(bv)** in interacinar spaces, **(D):** Group III showing parts of prostatic acini **(a)** are lined with thickened epithelium **(double arrows)**, papillary projections **(green arrows)** and some acini have pyknotic nuclei **(red arrow**) with vacuolated cytoplasm (*) and dilated blood vessels **(bv)** can be seen in interacinar spaces , **(E):** Group IV showing parts of prostatic acini **(a)** are lined with thickened epithelium **(double arrows)**, papillary projections **(green arrows),** inflammatory cellular infiltration **(if)** and dilated congested blood vessels **(bv)** in interacinar spaces, **(F):** Group V showing nearly normal regular acini **(a)** are lined with simple cuboidal epithelium **(black arrow)** with rounded nuclei **(blue arrow),** acini are contained acidophilic prostatic secretions **(ps)** and blood vessels **(bv)** can be seen in interacinar spaces, **(G):** Group VI showing irregular prostatic acini **(a)** are lined with thickened epithelium **(double arrows),** papillary projection **(green arrows),** stratification with narrow lumen **(n)** and blood vessels **(bv)** can be seen in interacinar spaces **(H&E X400).**

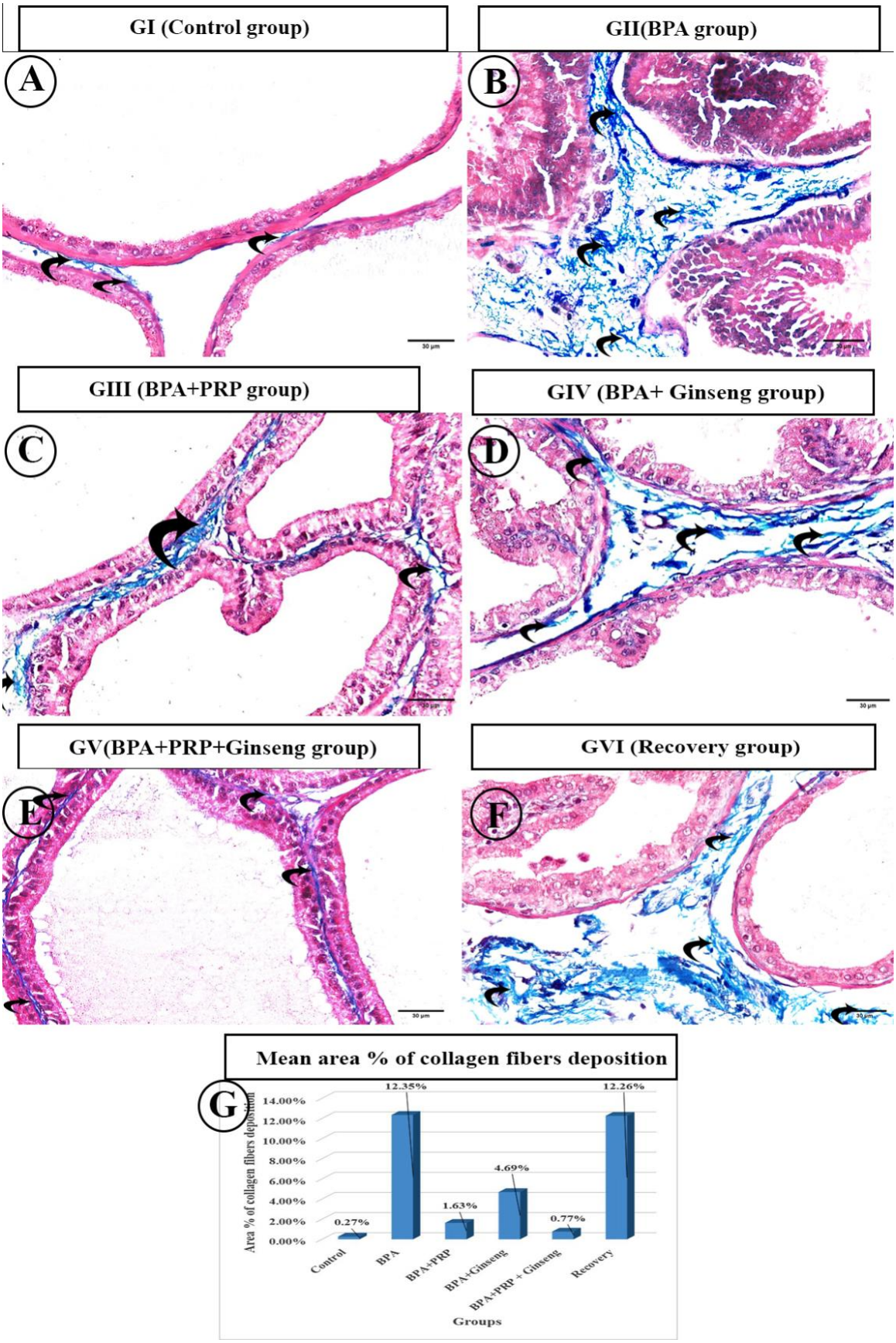
GI (Control group)
GII(BPA group)
A
B
GIII (BPA+PRP group)
GIV (BPA+ Ginseng group)
C
D
GV(BPA+PRP+Ginseng group)
GVI (Recovery group)
E
F
Mean area % of collagen fibers deposition
G
Area % of collagen fibers deposition
14.00%
12.00%
10.00%
8.00%
6.00%
4.00%
2.00%
0.00%
0.27%
12.35%
1.63%
4.69%
0.77%
12.26%
Control
BPA
BPA+PRP
BPA+Ginseng
BPA+PRP + Ginseng
Recovery
Groups

Fig. 2: Photomicrographs of rat prostatic sections stained with Masson's trichrome (X400), showing collagen fibers deposition patterns in between the prostatic acini (arrows): (A): Minimal deposition of collagen fibers in control group, **(B):** Intense deposition of collagen fibers in group II, **(C):** Mild deposition of collagen fibers in group III, **(D):** Moderate deposition of collagen fibers in group IV, **(E):** Minimal deposition of collagen fibers in group V, **(F):** Marked deposition of collagen fibers in group VI, **(G):** A histogram showing the mean area % of collagen fibers deposition in all groups.

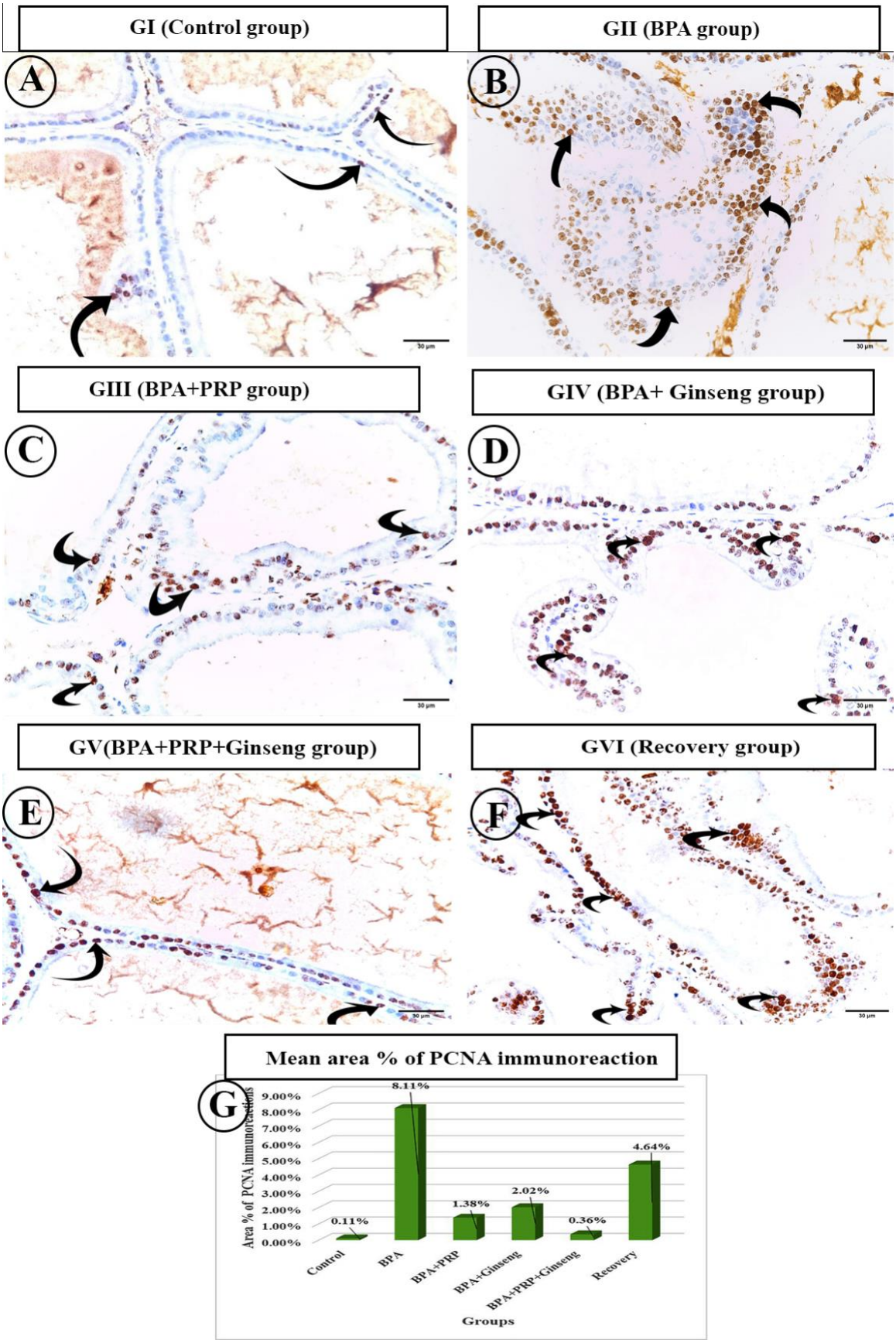
GI (Control group)
GII (BPA group)
A
B
GIII (BPA+PRP group)
GIV (BPA+ Ginseng group)
C
D
GV(BPA+PRP+Ginseng group)
GVI (Recovery group)
E
F
Mean area % of PCNA immunoreaction
G
Area % of PCNA immunoreactions
9.00%
8.00%
7.00%
6.00%
5.00%
4.00%
3.00%
2.00%
1.00%
0.00%
0.11%
8.11%
1.38%
2.02%
0.36%
4.64%
Control
BPA
BPA+PRP
BPA+Ginseng
BPA+PRP+Ginseng
Recovery
Groups

Fig. 3: Photomicrographs of rat prostatic sections immunostained for PCNA (X400), illustrating the percentage of brown nuclear PCNA immunoreactivity across groups (arrows): (A): Minimal positive PCNA immunoreaction in control group, **(B):** Intense positive PCNA immunoreaction in group II, **(C):** Mild positive PCNA immunoreaction in group III, **(D):** Moderate positive PCNA immunoreaction in group IV **(E):** Minimal positive PCNA immunoreaction in group V**, (F):** Marked positive PCNA immunoreaction in group VI, **(G):** A histogram showing the mean area % of PCNA immunoreaction in all groups.

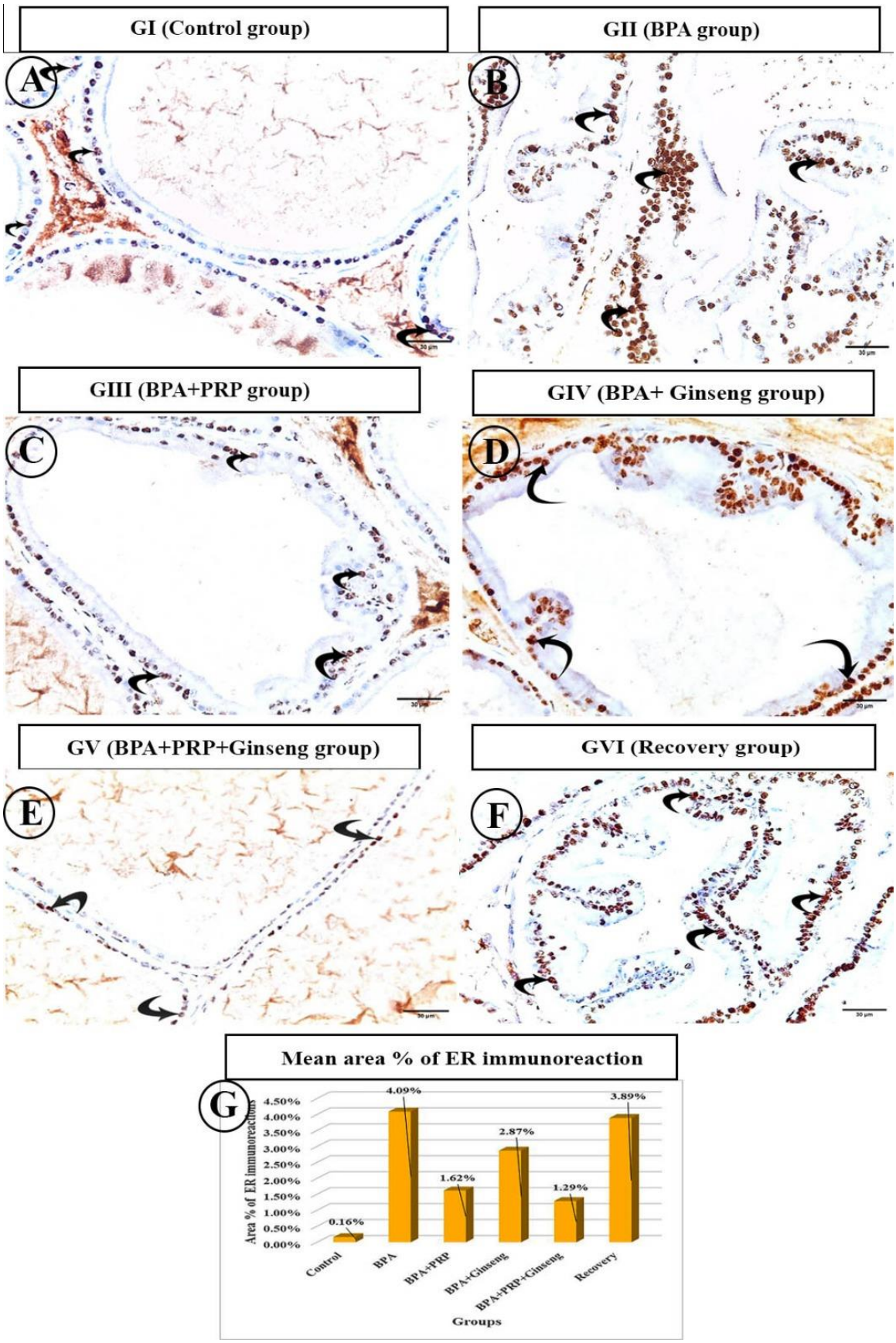
GI (Control group)
GII (BPA group)
A
B
GIII (BPA+PRP group)
GIV (BPA+ Ginseng group)
C
D
GV (BPA+PRP+Ginseng group)
GVI (Recovery group)
E
F
Mean area % of ER immunoreaction
G
Area % of ER immunoreactions
4.50%
4.00%
3.50%
3.00%
2.50%
2.00%
1.50%
1.00%
0.50%
0.00%
0.16%
4.09%
1.62%
2.87%
1.29%
3.89%
Control
BPA
BPA+PRP
BPA+Ginseng
BPA+PRP+Ginseng
Recovery
Groups

Fig. 4: Photomicrographs of rat prostatic sections immunostained for ER (X400), illustrating the percentage of brown nuclear ER immunoreactivity across groups (arrows): (A): Minimal positive ER immunoreaction in control group, **(B):** Intense positive ER immunoreaction in group II, **(C):** Mild positive ER immunoreaction in group III, **(D):** Moderate positive ER immunoreaction in group IV **(E):** Minimal positive ER immunoreaction in group V**, (F):** Marked positive ER immunoreaction in group VI, **(G):** A histogram showing the mean area % of ER immunoreaction in all groups.